Air-Sea Exchanges of Fresh Water: Global Oceanic Precipitation Analyses

Pingping Xie[1], John Janowiak[1] and Phillip Arkin[2]
[1] NOAA Climate Prediction Center, Camp Springs, MD
[2] Earth Systems Science Interdisciplinary Center, University of Maryland, College Park, MD

1. PROJECT SUMMARY

Oceanic Fresh water flux is an essential component of the global water cycle and plays an important role in forcing the oceanic circulation. However, its mean state, short-term variability and long-term changes are poorly monitored and documented due to undesirable qualities of the data sets for its two primary components, precipitation (P) and evaporation (E). Two major factors restricting the quality of existing oceanic fresh water flux data sets are 1) the lack of an extensive and continuous network of in-situ observations for calibrating and verifying each component, and 2) insufficient efforts to synthesize analyses for E and P. The availability of many new observation-based and model-produced data sets, especially precipitation, surface air temperature, sea surface temperature, humidity, and wind, makes it possible to quantitatively calibrate, verify and refine the existing P and E products.

In the past decade, two sets of satellite-based precipitation products have been developed at NOAA Climate Prediction center (CPC) and used to monitor precipitation variations over global oceans. The CPC Merged Analysis of Precipitation (CMAP, Xie and Arkin 1997) is defined by merging individual products of satellite estimates derived from infrared (IR) and microwave (MW) observations. The CMAP data sets are created on a 2.5^{o}lat/lon grid over the globe and on monthly and pentad (5-day) time resolution for a 27-year period from January 1979 to the present. The other CPC oceanic precipitation analysis is that generated by the CPC Morphing Technique (CMORPH, Joyce et al. 2004) for high temporal / spatial applications. Cloud/precipitation movement vectors are first computed from high-resolution infrared image data in 30-min intervals observed by geostationary satellites. These movement vectors are then used to 'move' the precipitation systems observed by the more-physically-based but less frequently sampled microwave observations in the time-space domain to get the analyzed fields of precipitation at the targeted times. The CMOPRH precipitation analysis is produced on an 8kmx8km grid over the globe from 60^{o}S to 60^{o}N and on 30-min intervals from December 2002. Both CMAP and CMORPH have been widely used by scientists around the world to a variety of applications including monitoring and assessment of global climate, model verifications and studies on global water budget/flux.

Further refinements of the CMAP and CMORPH are needed to improve their capacity to quantitatively document the precipitation variations and fresh water flux over the global oceans. The objectives of this project are to improve the CMAP and CMORPH precipitation analyses over ocean and to examine the fresh water flux as seen in the existing observations and in the NCEP Global Oceanic Data Assimilation System (GODAS). Specifically, we will

1) Provide the CMAP and CMORPH gridded analyses of oceanic precipitation, *together with estimates of uncertainty*, for a range of spatial and temporal scales consistent with data availability. Each product will be accompanied by a historical set of analyses of varying duration. The several products will be updated and made available to the various communities of interest as promptly as the availability of input data permit, with lags ranging from less than one day to 3 months.

2) Monitor and assess the global oceanic fresh water flux using our precipitation analyses several of the available oceanic evaporation products and compare them with that generated by the NCEP operational Global Oceanic Data Assimilation System (GDAS). As part of this activity, we will examine the uncertainty of the fresh water flux derived from the current generation of observed precipitation and evaporation analyses to get insight into to what extent the differences between the flux in GODAS and observation are attributable to problems of the model.

3) Perform a set of modular research and development tasks to address critical shortcomings of the current precipitation analyses and to improve the existing products.

2. FY 2006 ACCOMPLISHMENTS

2.1 CMAP Global Precipitation Analyses

This part of our research project involves two components: 1) documentation of the global oceanic fresh water flux using the CMAP precipitation analysis and observation-based data sets of evaporation; and 2) improvements of the current CMAP for better quantitative applications over ocean. In FY2006, we have examined the seasonal and interannual variations of the oceanic fresh water flux using observation-based data sets of CMAP monthly precipitation analysis and the Goddard Satellite-based Surface Turbulent Fluxes (GSSFC, Chou et al. 2003 and compared them with those used in the NCEP Reanalysis 2 for a 13-year period from 1988 to 2000. Fresh water flux generated by the NCEP Reanalysis 2 is used to drive the NCEP GODAS.

Global annual mean precipitation distribution (fig.1,top) is characterized by bands of strong precipitation associated with the Inter-Tropical Convection Zone (ITCZ) and South Pacific Convection Zone (SPCZ) over tropics and the storm tracks over extra-tropics. Maximum annual mean precipitation exceeding 10 mm /day is observed over western Pacific, while minimum amount of rainfall presents over oceanic dry zones over SE Pacific, SE Atlantic and oceanic regions west of Mexico and North Africa. NCEP Reanalysis 2 (fig.1, middle) reproduced the overall large-scale patterns of precipitation very well. Regional biases, however, are observed, with the Reanalysis 2 over- estimate precipitation over most of the oceanic regions except over coastal regions near maritime continent and northeast Asia and several other regions (fig.1, bottom).

Global distribution of annual mean evaporation (fig.2, top) has maxima at latitudes south and north of the ITCZ, respectively. Maximum annual mean evaporation of more than 6 mm/day appears over tropical central Pacific and Indian Ocean, while evaporation of limited quantity is observed over high latitude oceans and over coastal oceans near maritime continent. In general, the NCEP Reanalysis 2 captured the overall structure of the global evaporation depicted in the satellite-based GSSTF data set (fig.2, middle). The Reanalysis 2, however, tends to generate too much (too less) evaporation over western Pacific and Indian Ocean (eastern Pacific, South Oceans) (fig.2, bottom).

Combined, the NCEP reanalysis produces too much (less) fresh water flux (E-P) over central Pacific (Western Pacific and eastern Indian Ocean), providing the NCEP GODAS with a biased forcing field (fig.3). Correlation between the monthly anomaly of observed fresh water flux (E-P) and that in the Reanalysis 2 is low over tropics where exchange of fresh water components between ocean and atmosphere is most active (fig.4). These results suggest that fresh water flux used to force the current version of the NCEP / GODAS contains substantial errors and need to be improved in the future.

Part of the differences between the E-P in the observation and the Reanalysis 2 are attributable to the uncertainties in the observed precipitation (CMAP) and evaporation (GSSTF). To quantify the uncertainties, we have started to intercomparison various in-situ and satellite-based precipitation estimates, and, based on the intercomparison results, to refine the CMAP precipitation analysis. In FY06, we have

- Collected and processed precipitation estimates from several satellite and merged products. The data collection/processing activities are extremely time consuming and part of it is carried out jointly with the second part of this project on the improvements of CMORPH analysis;
- Performed brief comparisons of these satellite precipitation estimates to get insight into the overall structure of uncertainties in the observed precipitation with an emphasis on the systematic error; and
- Started examinations of evaporation data sets in several observed and modeled data sets (e.g. WHOI, NCEP Reanalysis 1); and
- Started development of the objective analysis technique used to generate the new CMAP analysis. The technique is based on the Optimal Interpolation (OI) technique of Gandin (1965) and combines information from multiple input sources based on their error structure.

2.2 CMORPH Global Precipitation Analyses

In this section, we address progress for each work item that was listed in the FY05 report.

- Development and integration of a decision model to determine when it is optimal to propagate precipitation using model winds rather than IR

We have developed three distinct ways to produce estimates of precipitation for each 30-minute period between overpasses by passive microwave sensors at a given location. One is to morph by using successive IR imagery to determine the motion of the precipitation field that has been identified and quantified by passive microwave data. The second method is to use NWP model winds instead of IR to morph the data. The third is to estimate precipitation directly from IR data. The issues are that morphing usually produced more accurate estimates of precipitation than estimates made from IR data, except when the time between microwave sensor overpasses is sufficiently long (about four hours). In addition, over the Tropics the use of mid-level model wind information to propagate the precipitation is often superior to using IR imagery to determine the motion of the precipitation field. Therefore, during FY06 we developed a decision model to determine which of these three estimates to use at any given location and time. This model was developed by withholding from the morphing process precipitation estimates that were derived from passive microwave data and using those data to validate morphed or IR-derived estimates at each 30-minute period between microwave overpasses.

- Development and implementation of an AMSU-B oceanic rainfall calibration method that increases detection frequency resulting in a better rain rate distribution.

The detection of oceanic rainfall is a problem for AMSU-B because the high frequency channels on that sensor have difficulty in detecting rainfall that is not associated with deep convection. Since "warm cloud" precipitation is not detectible by AMSU-B, overall the rainfall frequency of TMI is 2-3 times greater compared to the rainfall frequency derived by AMSU-B over oceanic areas (figure 5, top and middle panels respectively). Previously, since the CMORPH frequency matching calibration method conserves total rainfall relative to TMI, precipitation estimates derived from sensors or algorithms that suffer from rainfall detection deficiencies are adjusted upwards in regions where rainfall is detectable in order to match the larger rainfall area and hence total volume of the TMI-derived rainfall. Therefore, previously in oceanic regions where precipitation is detectable by the AMSU-B instrument, (convective regions primarily), the AMSU-B precipitation magnitude was adjusted heavier than TMI so that the rainfall volume per unit matches the TMI-derived estimates (not shown).

A new calibration method utilizes previously indeterminate AMSU-B retrievals to increase rainfall frequency of the AMSU-B instrument that nearly matches TMI. The oceanic AMSU-B rainfall detection in "warm rain" regions is improved (figure 5, bottom panel) by assigning the lightest rainfall rates possible to AMSU-B retrievals that are flagged because the ice water path (IWP) and effective diameter (De) do not "converge" (in the 0.05 - 3.0 Kg m-3 and 0.3 -3.5 mm respective ranges). An instantaneous case study depiction reveals the current NESDIS algorithm estimates higher rainfall in smaller regions relative to the TMI (figure 6, top and middle panels respectively). By assigning indeterminate retrievals the lightest remaining rainfall (figure 6, bottom panel), the new calibration procedure now produces a realistic characterization of rainfall in previously detected regions and while conserving total sensor estimated rainfall to the TMI

calibration standard. The scan angle dependent frequency matching calibration method will then be applied to this "expanded" AMSU-B rainfall.

- Determine the bias characteristics by comparing the CMORPH estimates with available in situ precipitation observations which will also assist in the development of error estimates (Figure 7).

As a first step, CMORPH estimates were used in conjunction with hourly rain gauge data from a dense network in southeastern China, to develop a bias reduction procedure. The procedure first interpolates the gauge data to match the CMORPH grid. Then, for each grid box that contains a rain gauge observation, we compute the ratio between the CMORPH and rain gauge estimates at each location over the previous 30 days (Gauge/CMORPH). Those ratios are then interpolated via the optimum interpolation (OI) method to obtain a spatially complete field of ratios. Then, at each grid box, the CMORPH value is multiplied by the appropriate ratio. The second step uses OI to integrate the rain gauge and bias corrected CMORPH data. Although this work is not directly relevant to oceanic precipitation, the methodology that was developed may be useful for CMORPH bias adjustment over the oceans by using coastal radars and buoy measurements of precipitation.

- Reprocess the entire CMORPH period of record using a frozen system in which all recent improvements have been incorporated

This task has been deferred to the next year, mainly because of the level of effort to derive the AMSU-B scan angle adjustment procedure, which we felt was necessary to have in place before beginning a reprocessing effort.

- Extend the CMORPH period of record back through January 2002 – perhaps further, depending upon the availability of inputs

In order to perform this task, it is necessary to retrieve precipitation estimates derived from passive microwave sensors (SSMI, AMSU-B, TMI, AMSR) in the form of "orbit by orbit" files. This is a substantial effort and considerable "data mining" was accomplished during FY06. To date, we have retrieved approximately 80-90% of the necessary passive microwave data from all available sources back to 1998.

3. PUBLICATIONS

Joyce, R. J. and R. R. Ferraro, 2006: Improvements of CMORPH resulting from limb adjustments and normalization of AMSU-B rainfall. 14th Conference on Satellite Meteorology and Oceanography
http://ams.confex.com/ams/Annual2006/techprogram/paper_104615.htm

Liang, J, and P. Xie, 2006: Toward the construction of a gauge-satellite merged analysis of hourly precipitation. 3rd International Precipitation Working Group Meeting. October 23 – 26, 2006, Melbourne, Australia.

4. REFERENCES:

Chou, S.-H., E. Nelkin, J. Ardizzone, R. Atlas, and C.-L. Shie, 2003: Surface turbulent heat and momentum fluxes over global oceans based on the Goddard satellite retrievals, version 2 (GSSTF2). *J. Climate*, **16**, 3,256-3,273.

Gandin, L.S., 1965: *Objective Analysis of meteorological fields.* Israel Program for Scientific Translations, 242pp.

Joyce, R.J., J.E. Janowiak, P.A. Arkin, and P. Xie, 2004: CMORPH: A method that produces global precipitation estimates from passive microwave and infrared data at high spatial and temporal resolution. *J. Hydrometeor.*, **5**, 487 – 503.

Xie, P., and P.A. Arkin, 1997: Global precipitation: A 17-year monthly analysis based on gauge observations, satellite estimates, and numerical model outputs. *Bull. Amer. Meteor. Soc.*, **78**, 2539 – 2558.

FIGURES:

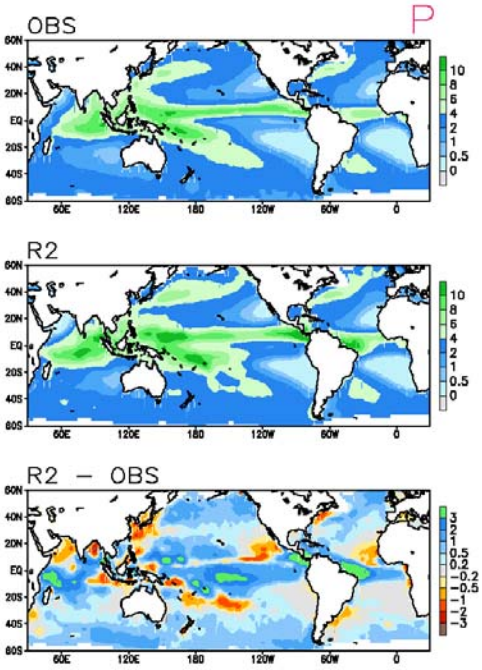

Fig. 1

Annual mean precipitation (mm/day) averaged over a 13-year period from 1988-2000, from the CMAP global precipitation analysis (OBS,top), the NCEP Reanalysis 2 (R2, middle), and the differences between them (bottom).

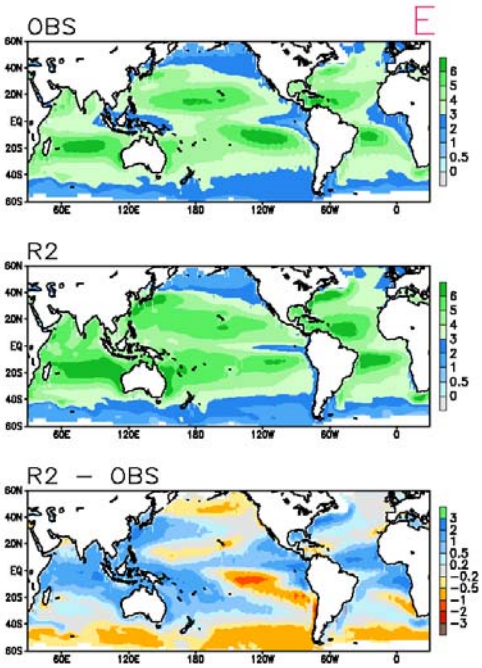

Fig. 2

Annual mean evaporation (mm/day) averaged over a 13-year period from 1988-2000, from the observation-based Goddard Satellite-based Surface Turbulent Fluxes (GSSTF, Chu et el. 2003, top), the NCEP Reanalysis 2 (middle), and the differences between them (bottom).

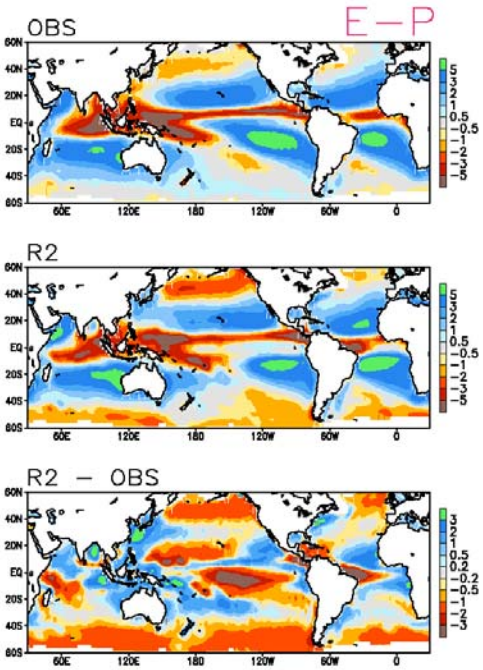

Fig. 3

Annual mean fresh water flux (E-P, mm/day) averaged over a 13-year period from 1988-2000, from the observation (OBS, top), the NCEP Reanalysis 2 (R2, middle), and the differences between them (bottom).

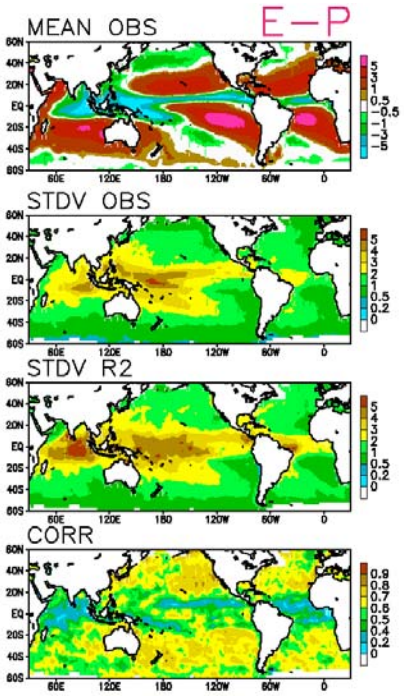

Fig. 4

Spatial distribution of mean E-P in the observation (top), standard deviation of E-P in the observation (2nd from top), standard deviation of E-P in the NCEP Reanalysis 2 (3rd from top), and correlation between monthly E-P anomaly in the observation and that in the Reanalysis 2 (bottom). Statistics are

calculated over a 13-year period from 1988 to 2000.

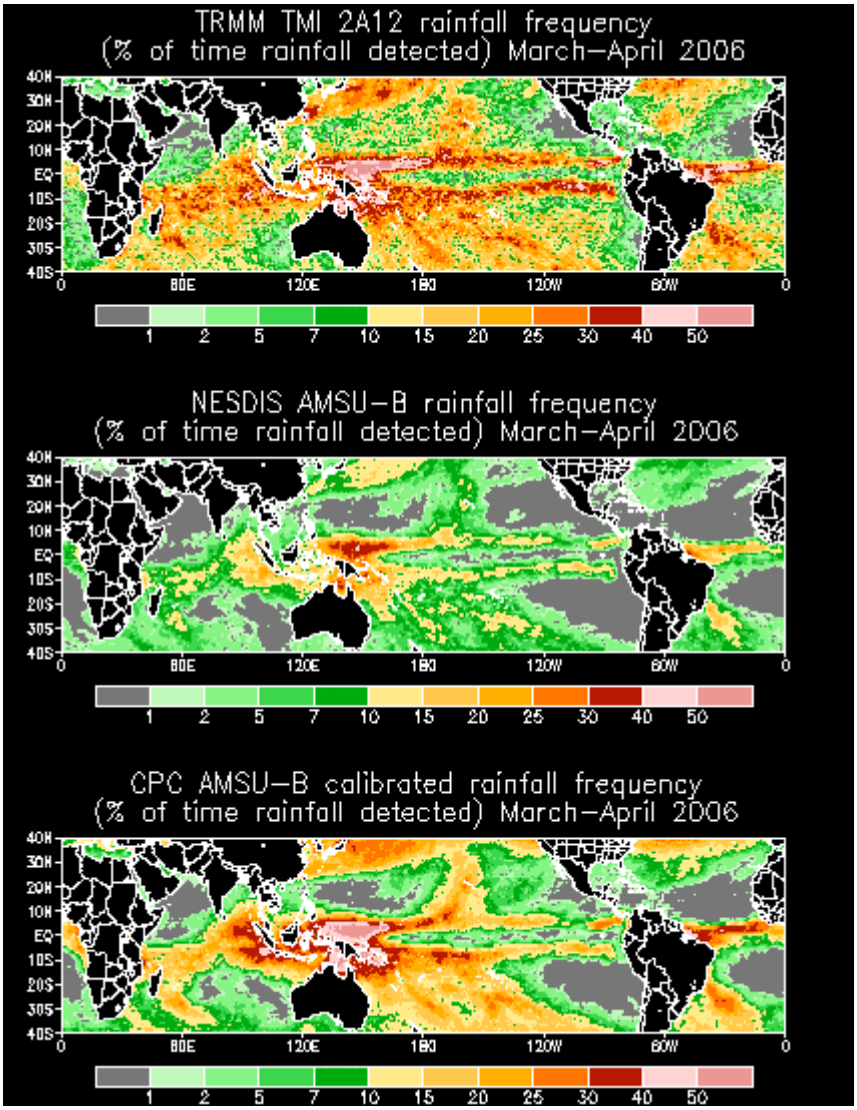

Figure 5. Comparison of precipitation frequency from the TRMM TMI 2A12 (top), unadjusted AMSU-B algorithm (middle), and the adjusted AMSU-B (bottom) for March – April 2006.

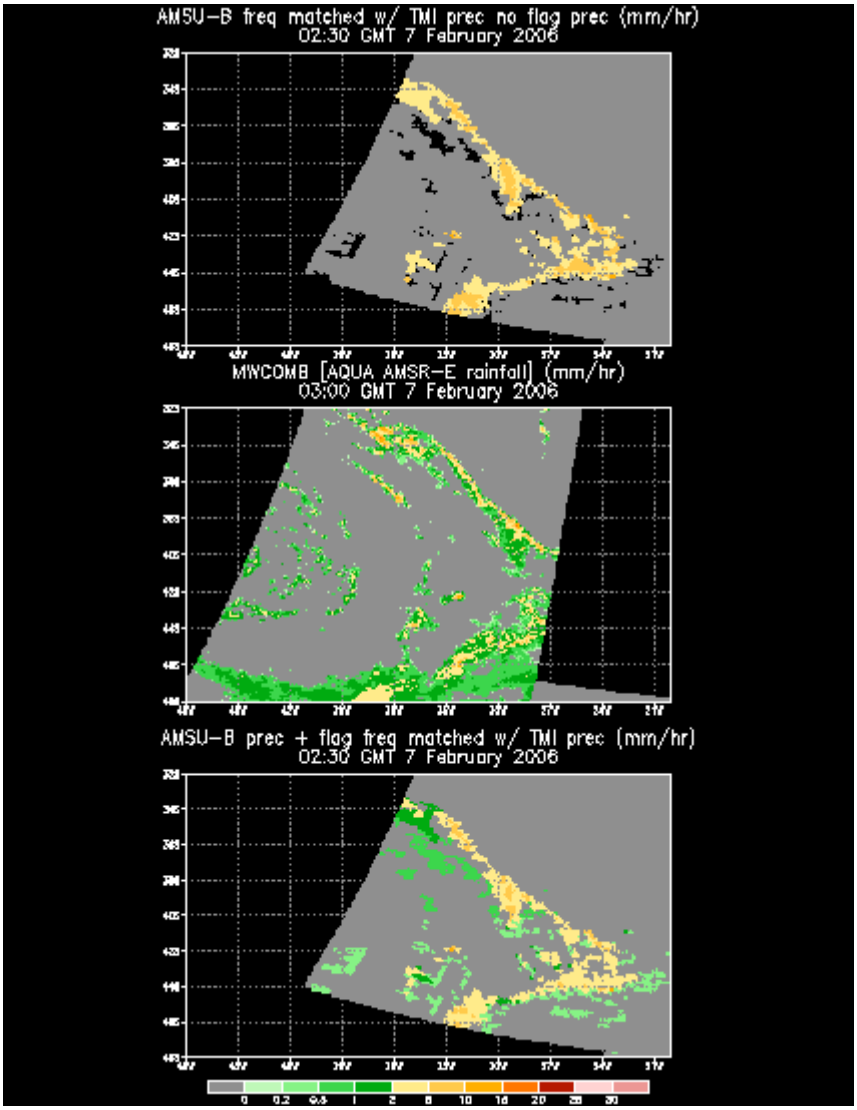

Figure 6. Comparison of instantaneous precipitation from the unadjusted AMSU-B NESDIS algorithm (top), TRMM TMI sensor (middle), and the calibrated AMSU-B algorithm (bottom).

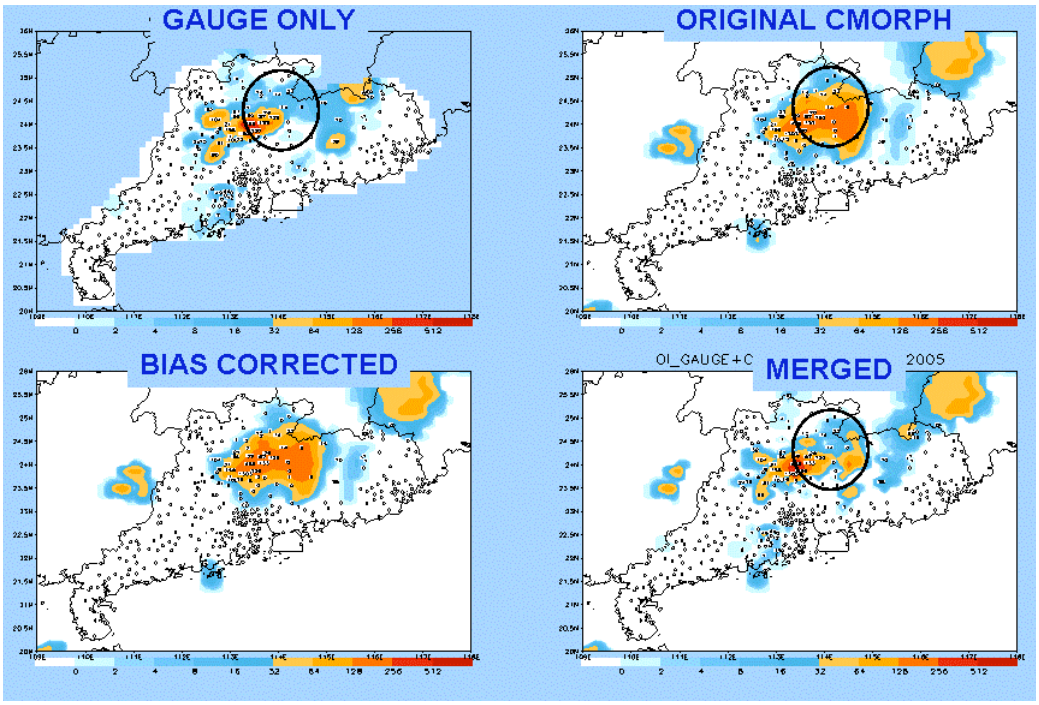

Figure 7. Example result of bias-adjustment procedure applied to CMORPH precipitation estimates. Rain gauge locates are denoted by dots. Note the circled areas in three of the panels, where CMORPH (upper-right) is high compared to the gauge analysis (upper-left) but that rain gauges are sparse in the region. The CMORPH/rain gauge merged analysis (lower-right) gives more weight to CMORPH (after bias adjustment) in gauge-sparse locations.